Measurement of the CR energy spectrum above 10^{18} eV with the Pierre Auger Observatory

P. Bernardini[1,3] C. Bleve[1,3,4], G. Cataldi[3], M. R. Coluccia[1,3], A. Corvaglia[3] P. Creti[3] S. D'Amico[2,3], I. De Mitri[1,3], U. Giaccari[1,3,6], G. Marsella[2,3], D. Martello[1,3], M.Panareo[2,3], L.Perrone[2,3], C. Pinto[3], F. Salamida[7], M. Settimo[1,3,5] and the Pierre Auger Collaboration

[1] Dipartimento di Fisica Università del Salento, Italy
[2] Dipartimento di Ingegneria dell'Innovazione Università del Salento, Italy
[3] Istituto Nazionale di Fisica Nucleare sez. di Lecce, Italy
[4] now at the Dept. of Physics, Bergische Universität Wuppertal, Germany
[5] now at the Dept. of Physics, University of Siegen, Germany
[6] now at Dipartimento di Fisica, Università Federico II di Napoli, Italy
[7] now at INPO, Orsay (France)

1. Introduction

In this paper, based on [1], we present an updated measurement of the cosmic ray energy spectrum with the Pierre Auger Observatory [2]. An accurate measurement of the cosmic ray flux above 10^{18} eV is a crucial aid for discriminating between different models describing the transition between galactic and extragalactic cosmic rays, the suppression induced by the cosmic ray propagation and the features of the injection spectrum at the sources.

Two complementary techniques are used at the Pierre Auger Observatory to study extensive air showers initiated by ultra-high energy cosmic rays (UHECR): a *surface detector array* (SD) and a *fluorescence detector* (FD).

The SD consists of an array of over 1600 water Cherenkov detectors covering an area of about 3000 km^2 allowing the sampling of electrons, photons and muons in the air showers at ground level with an on-time of almost 100%. In addition the atmosphere above the surface detector is observed during clear, moonless nights by 27 optical telescopes grouped in 5 buildings. This detector is used to observe the longitudinal development of an extensive air shower by detecting the fluorescence light emitted by excited nitrogen molecules and the Cherenkov light induced by the particles in the shower. Details regarding the design and the status of the Observatory can be found elsewhere [3–5].

The energy spectrum at energies greater than 3×10^{18} eV has been derived using data from the surface detector array of the Pierre Auger Observatory. The analysis of air showers measured with the fluorescence detector that triggered at least one station of the surface detector array (i.e. *hybrid* events) enables measurements to be extended to lower energies. Despite the limited number of events due to the fluorescence detector on-time, the lower energy threshold and the good energy resolution of *hybrid* events allow us to measure the flux of cosmic rays down to 10^{18} eV in the energy region where the transition between galactic and extragalactic cosmic rays is expected [6–8].

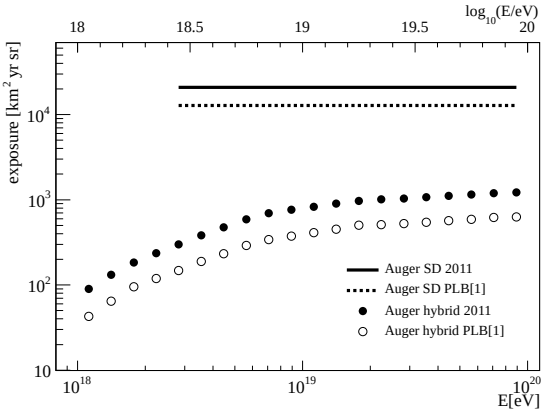

Figure 1. The SD and hybrid exposures used for the current flux measurement compared with a previously published data set [2]. The SD exposure is shown for energies higher than $10^{18.5}$ eV where the detector is fully efficient.

2. Surface detector spectrum

Here we report an update of the energy spectrum based on the surface detector data [2] using the period between 1 January 2004 and 31 December 2010. The exposure increased by about 60% with respect to the previous publication and is now 20905 km^2 sr yr. It is calculated by integrating the number of active detector stations of the surface array over time. The SD exposure is

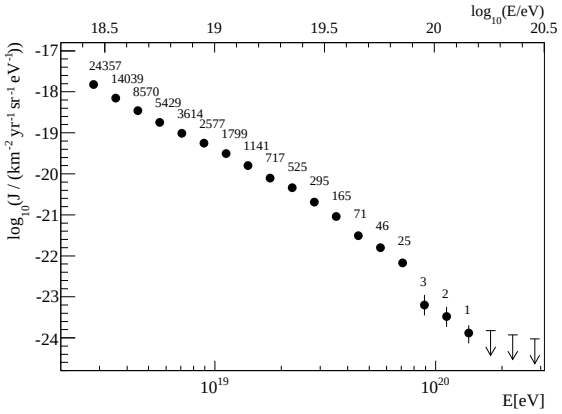

Figure 2. Energy spectrum derived from surface detector data calibrated with fluorescence detector measurements. The spectrum has been corrected for the energy resolution of the detector. Only statistical uncertainties are shown. Upper limits correspond to 68% CL.

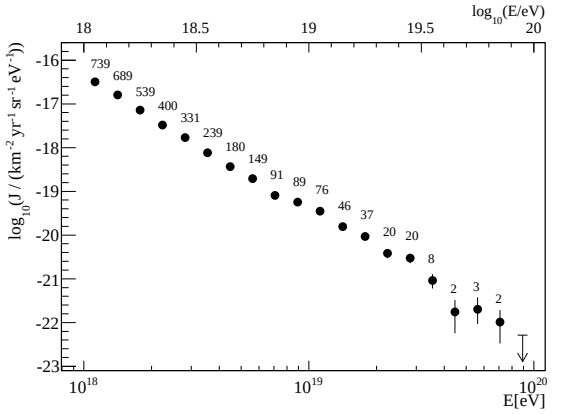

Figure 3. Energy spectrum derived from hybrid data. Only statistical uncertainties are shown. Upper limits correspond to 68% CL.

shown in Fig. 1 compared to the one used in [2]. Above 3×10^{18} eV the SD acceptance is saturated regardless of the primary mass. The uncertainty on the derivation of the exposure is about 3% [9].

The event selection requires the water-Cherenkov detector with the greatest signal to be surrounded by operational stations and the reconstructed zenith angle to be smaller than 60°. The total number of events above 3×10^{18} eV fulfilling the selection criteria is about 64000. The number of events with energy greater than 10^{19} eV is about 5000. The number of events above 3×10^{18} eV does not fully reflect the increase in exposure with respect to previous publication as the energy calibration has changed meantime [10].

As the energy estimator for the SD we use the expected signal at 1000 m from the shower core, corrected for shower attenuation effects. The calibration of the energy estimator of the surface detector is based on events measured in coincidence with the fluorescence detector [10]. The procedure is affected by a systematic error of 22% due to the uncertainty on the fluorescence energy assignment.

The energy resolution of the SD is ∼16% at threshold, falling to ∼12% above 10 EeV. Details can be found in [10]. The influence of the bin-to-bin migration on the reconstruction of the flux due to the energy resolution has been corrected by applying a forward-folding approach. The correction of the flux is mildly energy dependent but is less than 20% over the entire energy range.

The energy spectrum, including the correction of the energy resolution, is shown in Fig. 2. The number of events of the raw distribution is superimposed. The total systematic uncertainty of the flux for the derived spectrum is 6% and is obtained by summing in quadrature the exposure uncertainty (3%) and that due to the forward-folding assumptions (5%).

3. Hybrid energy spectrum

The energy spectrum from hybrid events is determined from data taken between 1 November 2005 and 30 September 2010. With respect to the previous publication [2] the time period has been extended and the events recorded at the site of the Loma Amarilla fluorescence building, the final set of telescopes brought into operation, have been added into the analysis. The resulting integrated exposure is doubled with respect to the previous publication [2,11]. To ensure good energy reconstruction only events that satisfy strict quality criteria have been accepted [11]. In particular, to avoid a possible bias in event selection due to the differences between shower profiles initiated by primaries of different mass, only showers with geometries that would allow the observation of all primaries in the range from proton to iron are retained in the data sample. The corresponding fiducial volume in terms of shower-telescope distance and zenith angle range is defined as a function of the reconstructed energy and has been verified with data [12]. A detailed simulation of the detector response has shown that for zenith angles less than 60°, every FD trigger above 10^{18} eV passing all the selection criteria is accompanied by a SD trigger of at least one station, independent of the mass or direction of the incoming primary particle [11].

The exposure of the hybrid mode of the Pierre Auger Observatory has been calculated using a time-dependent Monte Carlo simulation. The changing configurations of both fluorescence and

surface detectors are taken into account for the determination of the on-time of the hybrid system. Within a time interval of 10 min, the status and efficiency of all detector components of the Observatory, down to the level of the single PMTs of the fluorescence detector, are determined. Moreover, all atmospheric measurements [13] as well as monitoring information are considered and used as input for the simulation. A detailed description can be found in [11,14]. The longitudinal profiles of the energy deposits have been simulated with the CONEX [15] air shower simulation program with Sibyll 2.1 [16] and QGSJet II-0.3 [17] as alternative hadronic interaction models. The influence of the assumptions made in the hadronic interaction models on the exposure calculation has been estimated to be lower than 2%. A 50% mixture of protons and iron nuclei has been assumed for the primaries. The quality cuts used for the event selection lead to only a small dependence of the exposure on the mass composition. The systematic uncertainty arising from the lack of knowledge of the mass composition is about 8% (1%) at 10^{18} eV ($> 10^{19}$ eV). The full MC simulation chain has been cross-checked with air shower observations and the analysis of laser shots fired from the Central Laser Facility [18]. The total systematic uncertainty of the derived exposure is estimated as 10% (6%) at 10^{18} eV ($> 10^{19}$ eV).

The energy spectrum calculated using the hybrid events is shown in Fig. 3. The main systematic uncertainty is due to the energy assignment which relies on the knowledge of the fluorescence yield, choice of models and mass composition [19], absolute detector calibration [20] and shower reconstruction. The total uncertainty is estimated to be about 22%. The details can be found in [2].

4. Combined energy spectrum

The energy spectrum derived from hybrid data has been combined with the one obtained from surface detector data using a maximum likelihood method. Since the surface detector energy estimator is calibrated with hybrid events [10], the two spectra have the same systematic uncertainty in the energy scale (22%). On the other hand, the normalisation uncertainties are independent. They are taken as 6% for the SD and 10% (6%) for the hybrid flux at 10^{18} eV ($> 10^{19}$ eV). These normalisation uncertainties are used as additional constraints in the combination. This combination procedure is used to derive the scale parameters $k_{\rm SD}$=1.01 and $k_{\rm FD}$=0.99 which have to be applied to the individual spectra in order to match them.

The characteristic features of the combined spectrum have been quantified in two ways. For the first method, shown as a dotted line in Fig. 4, three power laws with free breaks between them have been used. For the second approach, two power laws in the ankle region and a smoothly changing function at higher energies have been adopted. The function is given by

$$J(E; E > E_{\rm ankle}) \;\propto\; E^{-\gamma_2}\,\frac{1}{1+\exp\left(\frac{\lg E - \lg E_{1/2}}{\lg W_c}\right)},$$

where $E_{1/2}$ is the energy at which the flux has fallen to one half of the value of the power-law extrapolation and W_c parameterizes the width of the transition region. The result of the fit is shown as black solid line in Fig. 4. The derived parameters quoting only the statistical uncertainties are given in Table 1. Changes to the calibration curve [10] have resulted in some changes of the parameters of the spectrum with respect to previous work [2], although only the values of γ_2 are different by more than the quoted statistical uncertainties (in Ref. [2] a value of

Table 1
Fitted parameters and their statistical uncertainties characterizing the combined energy spectrum.

parameter	broken power laws	power laws + smooth function
$\gamma_1 (E < E_{\rm ankle})$	3.27 ± 0.02	3.27 ± 0.01
$\lg(E_{\rm ankle}/{\rm eV})$	18.61 ± 0.01	18.62 ± 0.01
$\gamma_2 (E > E_{\rm ankle})$	2.68 ± 0.01	2.63 ± 0.02
$\lg(E_{\rm break}/{\rm eV})$	19.41 ± 0.02	
$\gamma_3 (E > E_{\rm break})$	4.2 ± 0.1	
$\lg(E_{1/2}/{\rm eV})$		19.63 ± 0.02
$\lg(W_{\rm c}/{\rm eV})$		0.15 ± 0.02
χ^2/ndof	$37.8/16 = 2.7$	$33.7/16 = 2.3$

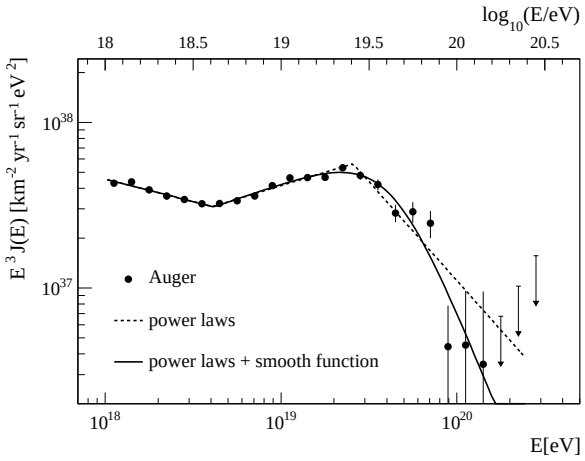

Figure 4. The combined energy spectrum is fitted with two functions (see text). Only statistical uncertainties are shown. The systematic uncertainty in the energy scale is 22%.

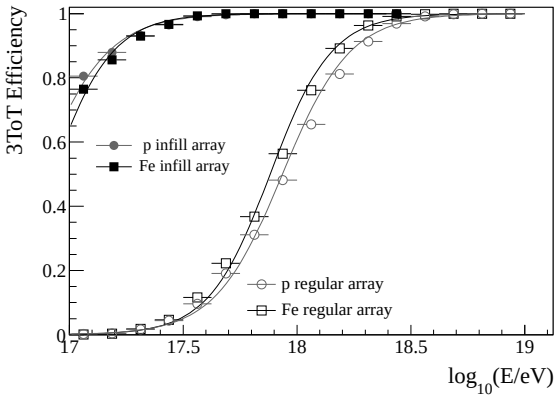

Figure 5. 3ToT trigger efficiency for the infill and regular array obtained from simulations of Iron and proton primaries.

$\gamma_2 = 2.59 \pm 0.02$ is reported).

5. Towards the lower energies

The energy range between 10^{17} eV and $4{\times}10^{18}$ eV is of great interest for understanding the origin of cosmic rays. At these energies the transition from the galactic to extragalactic accelerators [6] is expected. Also a spectral feature caused by the drop of the heavy component of the galactic cosmic rays [22] has been predicted. To extend the measurements to lower energies two enhancements are being built: HEAT [23] (High Elevation Auger Telescopes) and AMIGA (Auger-Muons and Infill for the Ground Array) [24]. The 61 detectors of the infill array are on a triangular grid with a spacing of 750 m. The trigger system of the infill array is adopted from the regular Auger array. An event is accepted when at least 3 stations forming a triangle satisfy a local trigger of the type Time-over-Threshold (3ToT event) [25]. The smaller spacing between stations of the infill lead to an increase of the trigger efficiency at low energy. The trigger efficiency as a function of energy for 3ToT events with zenith angles below 55° is illustrated in Fig 5, for both infill and regular array. The calculation is based on the parametrization of the single station lateral trigger probability [26], which reflects the properties of the station response and of the airshower development. The performance and current status of the analysis of the data taken with the infill array and with AMIGA are discussed in detail in [27].

REFERENCES

1. F. Salamida for the Pierre Auger Collaboration, Proc. 32st ICRC, Beijing, China, 2011, arXiv:1107.4809[astro-ph]
2. The Pierre Auger Collaboration, Phys. Lett., 2010, **B685**:239-246.
3. The Pierre Auger Collaboration, Nucl. Instr. and Meth., 2004, **A523**:50-95.
4. I. Allekotte et al., Nucl. Instr. and Meth., 2008, **A586**:409-420.
5. The Pierre Auger Collaboration, Nucl. Instr. and Meth., 2010, **A620**:227-251.
6. V. Berezinsky, A. Z. Gazizov, and S. I. Grigorieva, Phys. Lett., 2005, **B612**:147-153.
7. A. M. Hillas, J. Phys., 2005, **G31**:R95-R131.
8. T. Wibig and A. W. Wolfendale, J. Phys., 2005, **G31**:255-264.
9. The Pierre Auger Collaboration, Nucl. Instr. and Meth., 2010, **A613**:29-39.
10. R. Pesce for the Pierre Auger Collaboration, Proc. 32st ICRC, Beijing, China, 2011, arXiv:1107.4809[astro-ph]
11. The Pierre Auger Collaboration, Astropart. Phys., 2011, **34**:368-381.
12. The Pierre Auger Collaboration, Astropart. Phys., 2007, **27**:155-168.
13. K. Louedec for the Pierre Auger Collaboration, Proc. 32st ICRC, Beijing, China, 2011, arXiv:1107.4806[astro-ph]
14. S. Argiró et al., Nucl. Instr. and Meth., 2007, **A580**:1485-1496.
15. T. Bergmann et al., Astropart. Phys., 2007, **26**:420-432.
16. E. Ahn, R. Engel, T. K. Gaisser, P. Lipari, T. Stanev, Phys. Rev., 2009, **D80**:094003.
17. S. Ostapchenko, Nucl. Phys. B (Proc. Suppl.), 2006, **151**:143-146.
18. The Pierre Auger Collaboration, Astropart. Phys., 2010, **33**:108-129.
19. T. Pierog, R. Engel, D. Heck, S. Ostapchenko, K. Werner, Proc. 30th Int. Cosmic Ray Conf. (Merida, Mexico), 2007, **4**:625-628.
20. R. Knapik for the Pierre Auger Collaboration, Proc. 30th Int. Cosmic Ray Conf. (Merida, Mexico), 2007, **4**:343-346.
21. R.U. Abbasi, et al. (HiRes Collaboration), Astropart. Phys., 2009, **32**:53-60.
22. J.R. Hörandel, Astropart. Phys.,2003, 19(2):193
23. H.J. Mathes for the Pierre Auger Collaboration, Proc. 32st ICRC, Beijing, China, 2011, arXiv:1107.4807[astro-ph]
24. F. Sanchez for the Pierre Auger Collaboration, Proc. 32st ICRC, Beijing, China, 2011, arXiv:1107.4807[astro-ph]
25. The Pierre Auger Collaboration, Nucl. Instrum. Meth. in Phys., 2010, A 613:29
26. The Pierre Auger Collaboration, Astropart. Phys. 35 (2011) 266
27. I. Maris for the Pierre Auger Collaboration, Proc. 32st ICRC, Beijing, China, 2011, arXiv:1107.4809[astro-ph]